Scientific Journal of King Faisal University:
Basic and Applied Sciences

Magneto-Exciton Energy in Cylindrical Indium Arsenide Quantum Dots Affected by External Parameters

Marwan Zuhair Elias
Department of Medical Physics, College of Science, Mosul University, Mosul, Iraq

LINK	RECEIVED	ACCEPTED	PUBLISHED ONLINE	ASSIGNED TO AN ISSUE
https://doi.org/10.37575/b/sci/250014	11/04/2025	27/05/2025	27/05/2025	01/06/2025
NO. OF WORDS	**NO. OF PAGES**	**YEAR**	**VOLUME**	**ISSUE**
3491	5	2025	26	1

ABSTRACT

The effects of temperature, pressure, and an applied magnetic field on the energies of a cylindrical layer of indium arsenide (InAs) quantum dots, with and without Coulomb interaction, are investigated. Exciton energy depends significantly on these parameters. The results show that the ground-state and excited-state energies increase with rising temperature and applied magnetic field (blue shift), but that both energy states decrease with increasing pressure (red shift). As the temperature increases for higher states, the sensitivity of magneto-exciton energy also increases. The outcomes obtained for layered and ring-shaped systems exhibit a universal quality, making them particularly interesting.

KEYWORDS
Exciton, magnetic field, nanostructures, potential, pressure, temperature

CITATION
Elias, M.Z. (2025). Magneto-exciton energy in cylindrical indium arsenide quantum dots affected by external parameters. *Scientific Journal of King Faisal University: Basic and Applied Sciences*, **26**(1), 64–8. DOI: 10.37575/b/sci/250014

1. Introduction

The fact that motion in zero-dimensional semiconductor structures is limited in all three dimensions and that their sizes are smaller than or equivalent to the bulk exciton Bohr radius has attracted significant attention. Over the past 20 years, a large number of studies have been published on the creation and decay of exciton states in nanostructures containing quantum dots (QDs), as well as on how these states interact with other quasiparticles and external fields.

Core/shell nanomaterials may be constructed primarily as a result of recent technological advancements in material growth processes; these materials' unique and improved optical and electrical characteristics make them extremely desirable from an application standpoint. The confinement of quasiparticle motion in QDs leads to an increase in binding energy (BE), oscillator strength, and exciton lifetime in such systems (Kramar, 2009).

Numerous works have addressed the topic of determining the energy and BE of an exciton in nanostructures with QDs; an imperfect list of these works is provided by Elias (2019). Bhat and Shah (2018) presented findings on exciton energies in spherical gallium arsenide (GaAs) QDs, showing that dot size affects exciton energies and that the initial excited-state exciton energy becomes five orders of magnitude larger than the ground-state exciton energy for a consistent dot radius.

Pokutnyi (2013) investigates a quasi-zero-dimensional semiconductor nano system where an electron is restricted to the outer spherical boundary between the QD and dielectric matrix while a hole navigates through the QD volume. The system produces ground-state exciton BE that exceeds the values found in zinc selenide and cadmium sulfide single crystals.

Chafai *et al.*, 2019 studied the effects an external electric field has on the exciton energy spectrum in spherical GaN/AlN core/shell nanodots. They examined how an external electric field modifies the energy spectrum of excitons. This study also considers how changes in nanodot size influence the lowest energy state of confined excitons. According to a theoretical model using variational computation, the exciton energy experiences a significant reduction when the electric field is applied. The study shows that a specific energy red shift exists between the intensity of the external electric field and specific sizes of nanodots. Further research demonstrates that increases in nanodot size lead to a decrease in the lowest exciton energy, while decreases in nanodot size result in higher, lowest exciton energy.

Pokytnyi *et al.*, (2023) studied exciton quasi-molecules existing in germanium double QDs situated in a silicon matrix nano system. When two spatially indirect excitons interact, they combine to form an exciton quasi-molecule. The production of spatially indirect excitons and exciton quasi-molecules in the nano system was shown to depend on the distance D between QD surfaces. The exciton quasi-molecule's singlet ground state exhibits BE greater than the biexciton BE in a silicon crystal by two orders of magnitude.

Standard QD confinement behavior is primarily determined by the nano system's average size as well as its composition. Zieliński *et al.* (2015) reveal that natural QDs produced in the indium arsenide (InAs)/GaAs wetting layer have their excitonic properties predominantly determined by random lattice composition fluctuations. The biexciton BE shows extreme sensitivity to lattice randomness while exhibiting almost no dependency on exciton energy.

The notable flexibility of TMDC materials permits strain to alter their fundamental exciton energies and spectral linewidths. Niehues *et al.*, 2020 provided a description of the Stokes shift, which represents the energy difference between light absorption and emission for the A exciton in TMDC mono- and bilayers. Research indicates that mechanical strain enables tuning of the Stokes shift. The Stokes shift diminishes as tensile strain levels increase. The interaction between excitons and phonons weakens due to shifts in the energy positions of various excitons.

Iris Niehues *et al.*, (2019) investigated how interlayer excitons in bilayer MoS_2 respond to uniaxial tensile strain up to a maximum of 1.6%. They measured a gauge factor of −47 meV per percent through differential transmission spectra at varying strain levels, which track the energy shift in the interlayer exciton. The intralayer A and B excitons display a gauge factor of −49 meV per percent. Their research confirms that

Corresponding Author: Marwan Zuhair Elias 009647702028210, marwanzuhairelias.1001@gmail.com

interlayer excitons originate at the K point of the Brillouin zone, where the electron remains within a single layer while the hole extends across two layers. This work creates potential opportunities for future straintronic devices utilizing interlayer excitons.

The authors explored the exciton configuration in type II QDs, where the hole resides in the barrier material and the electron remains inside the dot (Janssens *et al.*, 2001a). The Hartree–Fock mesh computation method evaluates exciton properties under a perpendicular magnetic field. A flat quantum disk serves as one component within the simulation system. Angular momentum transitions are expected to occur as the magnetic field increases. Their research analyzes how modifications in the hole's confinement potential lead to the transformation of a type I QD into a type II QD. Under strong magnetic field conditions, a re-entrant behavior emerges, resulting in a transition from type II back to type I behavior.

An exciton within a quantum disk displays ground-state energy and BE that vary with changes in the external magnetic field (Janssens *et al.*, 2001b). The confinement is modeled as a rigid wall with a finite height limitation. The study examines the diamagnetic shift when magnetic fields reach 40 T. When the light hole participates in exciton generation, researchers find strong agreement between their results and experimental data for InyAl1-yAs/AlxGa1−xAs self-assembled QDs. They analyzed the impact of dot size on the diamagnetic shift by varying the radius of the disk. Magnetic field-dependent exciton excited states were successfully identified. Since the relative angular momentum depends on magnetic field strength, it cannot serve as a valid quantum number. The ground-state properties of an exciton in a self-assembled quantum disk under a perpendicular magnetic field are reported by Janssens *et al.*, (2004).

Hsiao *et al.*, (2024) created a 4×2 germanium QD ladder and employed it to investigate the transport and generation of excitons. The authors tuned the entire array into the single-hole regime and independently controlled all of the interdot tunnel couplings and on-site potentials to design the Hamiltonian system. They discovered a significant inter-channel Coulomb interaction while suppressing tunneling between channels.

A QD with light hole–heavy hole splitting and a strong, high-energy exciton was described Wang *et al.*, (2024). According to their experimental and computational data, the oscillator strength of heavy holes decreases more than that of light holes under electric fields. This, the authors argue, is the primary cause of the strong light-hole electroluminescence. Both $CdxZn_{1-x}Se$–ZnS and CdSe–CdS core–shell QDs with substantial light hole–heavy hole splitting show this phenomenon.

The size-dependent scintillation of $CsPbBr_3$ nanocrystals was investigated both theoretically and experimentally by Fratelli *et al.*, (2025), using a combination of spectroscopic, radiometric, and Monte Carlo simulation methods. Due to their higher stopping power and lower Auger decay, the results demonstrated that the combined effects of size-dependent energy deposition, (multi-)exciton population, and light emission under ionizing excitation—all characteristic of confined particles—serve to maximize the scintillation efficiency and timing performance of larger nanocrystals. This model offers essential guidance for the rational design of nanoscale scintillators.

The ability to create spatial variations in QDs, quantum wires, and quantum wells with various geometries forms a fundamental basis for understanding the theoretical framework behind layered and ring-shaped configurations. The system functions as a quantum well when the cylindrical nanolayer maintains a constant thickness while both inner and outer radii expand. A quantum wire is formed when the cylindrical quantum layer's inner radius vanishes and height approaches infinity. The structure becomes a cylindrical QD when the height remains fixed, and the inner radius disappears (Zuhair *et al.*, 2009; Barseghyan *et al.*, 2024; Zuhair, 2012). The results obtained for both layered and ring-shaped systems show universal characteristics that make them particularly interesting. The present study investigates how temperature, pressure, and magnetic field influence exciton states in cylindrical-layer QDs.

2. Theoretical Framework

The investigation of how pressure, temperature, and magnetic field affect the exciton energy of an InAs cylindrical layer QD requires calculations of electron quantized energy (E_n), well thickness (L), dot radii (R), effective electron mass (m^*), and energy correction (ΔE_0) based on these parameters. The single-particle states are examined within a cylindrical layer QD characterized by height L and inner and outer radii R_1 and R_2, respectively, as shown in Fig. 1. Given that the radial motion of an electron is confined between the inner and outer radii, both the wave function and energy spectrum are determined under the assumption of a uniform magnetic field along the OZ-axis. The layer's confinement potential is defined by infinitely tall rectangular walls:

$$v(\rho,z,p)=\begin{cases}0,\mathrm{R}_1(p)\le\rho\le\mathrm{R}_2(p),-\frac{\mathrm{L}}{2}\le z\le+\frac{\mathrm{L}}{2}\\ \infty\quad,\rho<\mathrm{R}_1(p),\rho>\mathrm{R}_2(p),|z|>\frac{L}{2}\end{cases}. \tag{1}$$

The corresponding Schrödinger equation, in terms of the parabolic dispersion law, takes the form:

$$\frac{1}{2m^*(p,t)}\left(\vec{P}(p,t)-\frac{e}{c}\vec{A}\right)^2\Psi(\rho,\emptyset,z,p,t)=E_n(\rho,\emptyset,z,p,t)\text{-}$$
$$.\Psi(\rho,\emptyset,z,p,t), \tag{2}$$

where $\vec{P}=\hbar k,\vec{A}=\frac{1}{2}\vec{r_l}\times\vec{B}$ is the vector potential. The effective mass of the electron in InAs, as a function of pressure and temperature, is given by:

$$m^*(p,t)=\left[1+\frac{15020}{E_g(p,t)}+\frac{7510}{E_g(p,t)+341}\right]^{-1}.m_0^*. \tag{3}$$

The bulk energy gap of InAs is provided by Duque *et al.*, (2006):

$$E_g(p,t)=\left(533+7.7.p-\frac{0.276.T^2}{T+83}\right). \tag{4}$$

The fractional change in the radii of the cylindrical layer QD is expressed as:

$$R_{1(2)}(p)=R_{1(2)}(0)(S_{11}+2S_{12}).P. \tag{5}$$

Here, $R_{1(2)}(0)$ denotes the zero-pressure inner (outer) radius, and the well thickness under pressure is:

$$L[P]=[L_0.((1-P.(S_{11}-2.S_{12})^{0.5}], \tag{6}$$

where L_0 is the original height of the well. The compliance constants S_{11} and S_{12} are given by:

$$S_{11}=\frac{\mathrm{C}_{11}+\mathrm{C}_{12}}{[(\mathrm{C}_{11}-\mathrm{C}_{12}).(\mathrm{C}_{11}+2\mathrm{C}_{12})]} \tag{7}$$

$$S_{12}=\frac{-C_{12}}{[(C_{11}-C_{12}).(C_{11}+2C_{12})]}, \tag{8}$$

where C_{11} and C_{12} are the elastic constants of InAs (Kita *et al.*, 2019). The wave function must satisfy the boundary conditions:

$$\psi(\pm L/2)=\psi(R_1)=\psi(R_2)=0. \tag{9}$$

The exact solution of Eq. (2) takes the following form:

$$\Psi(\rho,\emptyset,z,p,t)=\frac{1}{\sqrt{2\pi}}.e^{im\emptyset}.\sqrt{\frac{2}{L(P)}}.\begin{pmatrix}sin\frac{\pi n}{L(P)}Z\\ cos\frac{\pi n}{L(P)}Z\end{pmatrix}.G(\rho,p,t). \tag{10}$$

Substituting Eq. (10) into Eq. (2) yields a new equation for the function G(ρ,p,t):

$$\frac{\hbar^2}{2m^*(p,t)}\left(G(\rho,p,t)'' + \frac{1}{\rho}G(\rho,p,t)' - \frac{m^*(p,t)^2}{\rho^2}.G(\rho,p,t)\right) + \left[\varepsilon - E_n(\rho,\emptyset,z,p,t) - \frac{m^*(p,t).\omega_H^2.\rho^2}{8} - \frac{\hbar.\omega_H.m^*(p,t)}{2}\right].G(\rho,p,t) = 0 \quad (11)$$

where $\omega_H = e.H/m^*(p,t).c$ is the cyclotron frequency, and $E_n(\rho,\emptyset,z,p,t) = n^2\pi^2\hbar^2/2.m^*(p,t).L(P)$.

The simplest way to express the solution of Eq. (11) is using hypergeometric functions:

$$G(\rho,p,t) = \left\{c_1 F\left(-\left(\beta - \frac{|m^*(p,t)|+1}{2}\right), |m^*(p,t)|+1, \frac{\rho^2}{2a_H^2}\right) + c_2 U\left(-\left(\beta - \frac{|m^*(p,t)|+1}{2}\right), |m^*(p,t)|+1, \frac{\rho^2}{2a_H^2}\right)\right\}.e^{\frac{\rho^2}{4a_H^2}}.\rho^{|m^*(p,t)|}, \quad (12)$$

where $\beta = \frac{1}{\hbar\omega_H.(\varepsilon - E_n(\rho,\emptyset,z,p,t))} - \frac{m^*(p,t)}{2}$ and $a_H = \sqrt{\frac{\hbar}{m^*(p,t).\omega_H.}}$ represent the magnetic length.

Given that the wave function in Eq. (10) must vanish at the boundaries, the zero determinant condition $G(R_1) = G(R_2) = 0$ is required to determine the system's energy spectrum:

$$\begin{vmatrix} F\left(-\left(\beta - \frac{|m^*(p,t)|+1}{2}\right), |m^*(p,t)|+1, \frac{R_1^2}{2a_H^2}\right) & U\left(-\left(\beta - \frac{|m^*(p,t)|+1}{2}\right), |m^*(p,t)|+1, \frac{R_1^2}{2a_H^2}\right) \\ F\left(-\left(\beta - \frac{|m^*(p,t)|+1}{2}\right), |m^*(p,t)|+1, \frac{R_2^2}{2a_H^2}\right) & U\left(-\left(\beta - \frac{|m^*(p,t)|+1}{2}\right), |m^*(p,t)|+1, \frac{R_2^2}{2a_H^2}\right) \end{vmatrix} = \mathbf{0} \quad (13)$$

The energy spectrum is found by numerically solving the transcendental Eq. (13).

Now, using perturbation theory, the hole–electron interaction, or exciton effect, is examined under the assumption of strong quantization along the disk axis (OZ direction). Thus, in the present case, motion in the OZ direction is considered using the single-particle model (i.e., a two-dimensional exciton). The magneto-exciton Hamiltonian, in the limit of infinitely high walls, takes the following form:

$$\hat{H}_{ex} = \hat{H}_e + \hat{H}_h - \frac{e^2}{\varepsilon|\rho_e - \rho_h|}, \quad (14)$$

Where $\hat{H}_i = \frac{1}{m^*(p,t)}\left(\left(\hat{P}(p,t) - \frac{e}{c}\hat{A}_i\right)\right)$, (15)

and $\hat{H}_i.\Psi_i = E_i(\rho,\emptyset,z,p,t).\Psi_i$, where $(i = e = h)$.

In a first-order approximation, the magneto-exciton wave function can be expressed as:

$$\Psi_{ex}^0(r_e,r_h,p,t) = \Psi_e(\rho_e,\emptyset_e,z_e,p,t).\Psi_h(\rho_h,\emptyset_h,z_h,p,t). \quad (16)$$

This form assumes that the third term in Eq. (14) acts as a small perturbation to the Hamiltonian.

The corresponding energy correction is given by:

$$\Delta E_0 = \int \Psi_{ex}^0(r_e,r_h,p,t)\left(-\frac{e^2}{\varepsilon.\sqrt{\rho_e^2 - \rho_h^2 - 2\rho_e.\rho_h.\cos(\varphi_e - \varphi_h)}}\right)\Psi_{ex}^0.dv_e.dv_h. \quad (17)$$

Janssens *et al.*, (2002) state that this may be simplified to the following form:

$$\Delta E_0 = -\frac{8\pi e^2}{\varepsilon}.\int_{R_1(p)}^{R_2(p)}\rho_2.d\rho_2.\int_{R_1(p)}^{R_2(p)}\frac{f(\rho_1,\rho_2)}{\rho_1+\rho_2}.L\left(\frac{4\rho_1\rho_2}{(\rho_1+\rho_2)^2}\right)\rho_1.d\rho_2, \quad (18)$$

where $f(\rho_1,\rho_2) = \Psi_e^0(\rho_e,\emptyset_e,z_e,p,t).\Psi_h^0(\rho_e,\emptyset_e,z_e,p,t)$ and $L(x) = \int_0^{\pi/2}\frac{d\varphi}{\sqrt{1-x\sin^2(\varphi)}}$ is the complete elliptic integral of the first kind.

Thus, the total energy of the electron becomes:

$$E = E_e + E_h + \Delta E_0. \quad (19)$$

Figure 1: The cross-sectional area and specific features of the cylindrical layer quantum dot.

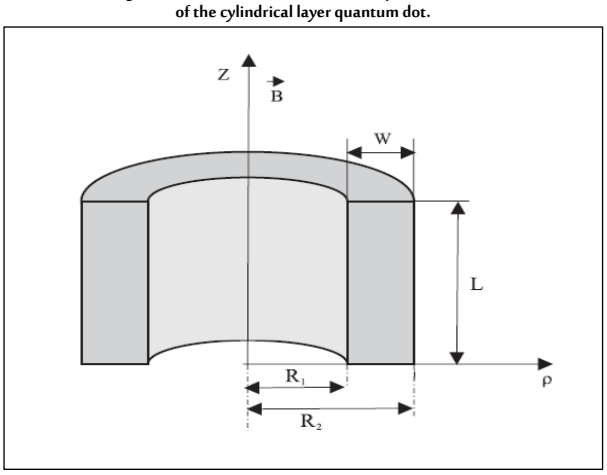

3. Analysis of the Results Obtained

Understanding how bound excitons respond to variations in external parameters is essential for the creation of tunable optical systems. The results of calculations for cylindrical InAs QDs are discussed for cases with and without Coulomb interaction. At given values of radii, pressure, and height, and under a perpendicular magnetic field directed along the OZ-axis, the energy of the exciton as a function of temperature is investigated, as shown in Fig. 2. Temperature influences the energy of excitons in cylindrical layer QDs (blue shift). As a result, the dependence of energy on temperature is found to be considerable.

Consequently, due to their interaction, electron–hole ground-state energy renormalization causes temperature-induced changes in exciton ground-state energy in QDs (Kramar, 2009). According to the observed results, nanostructured material properties may be controlled and altered through temperature via the band gap. In addition, due to their sensitivity to temperature, exciton behavior in nanostructures may be modified by adjusting the mobility and distribution of charge carriers (Zuhair, 2012). Furthermore, it is observed that at higher energy levels, relative to ground states, the sensitivity of exciton energy to temperature increases.

Figure 2: Energy (in meV) with and without Coulomb interaction versus temperature (in K) for different states at given values of radii, pressure, height, and magnetic field strength.

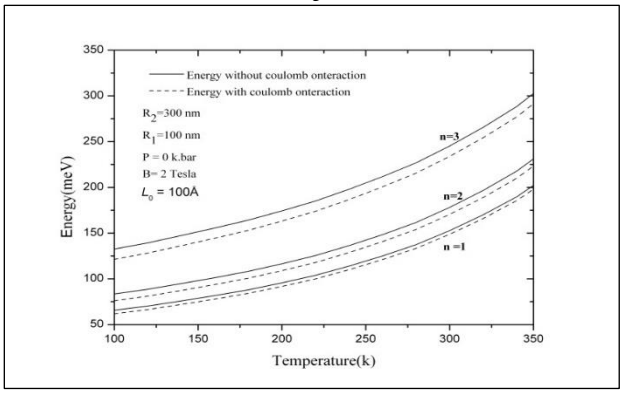

The impact of pressure on exciton energies trapped within a cylindrical QD made of InAs layers under a perpendicular magnetic field directed along the OZ-axis, for the cases with and without Coulomb interaction, is illustrated in Fig. 3. It is observed that energy is highly influenced by the applied pressure across all energy states (Bhat and Shah, 2018). Furthermore, according to Janssens *et al.*, (2004), as pressure increases, the hole moves from inside the dot to

its radial edge. This causes the BE between the electron and the hole to decrease, which, in turn, lowers the total energy.

Additionally, the results from comparing the ground-state and first excited-state curves for a given dot radius reveal that with increasing pressure, the exciton energy in the first excited state increases by approximately 25% more than the energy in the ground state.

Calculations performed for the ground-state energy as a function of the exciton's external magnetic field in InAs cylindrical layer QDs are presented in Fig. 4, considering fixed values of temperature, pressure, and radii for both cases—with and without Coulomb interaction. In good agreement with Janssens *et al.*, (2001b), the exciton ground-state energy rises under an externally applied magnetic field of up to 10 T. Additionally, it is observed that although the curves for both cases are almost parallel, the space between them gradually narrows as the magnetic field increases, in strong agreement with the findings of Ghosh *et al.*, 2024.

Figure 3: Energy (in meV) with and without Coulomb interaction versus pressure for different states at given values of radii, temperature, height, and magnetic field strength.

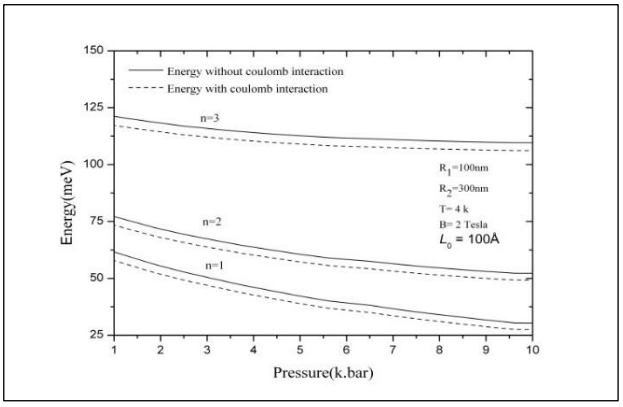

Figure 4: Exciton energy (in meV) with and without Coulomb interaction versus magnetic field strength for different states at given values of radii, pressure, temperature, and height.

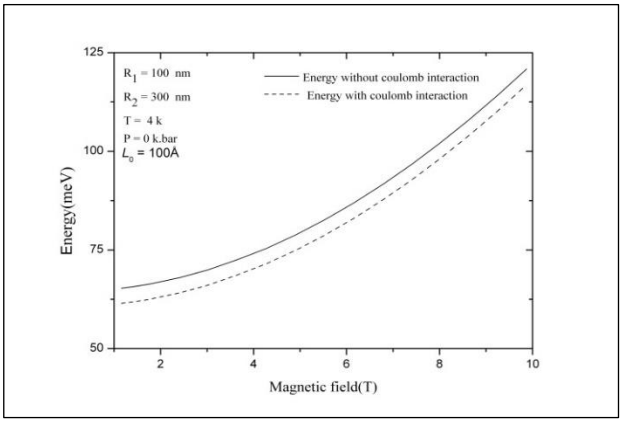

4. Conclusions

Creating layered-shaped nanostructures has led to the development of a new class of theoretical problems concerning the physical behavior of these systems, which is a noteworthy outcome. The present study examines the impact of external factors, such as temperature, pressure, and applied magnetic field, on the exciton energy of InAs cylindrical layer QDs. The findings show that, at a given dot size, energy increases with rising temperature and applied magnetic field but decreases with increasing pressure. These results have several applications in nanoelectronics and are significant from both applied and fundamental standpoints.

Data Availability Statement

The data supporting this study's findings are available on request from the corresponding author.

Acknowledgments

We extend our heartfelt thanks to the University of Mosul for its encouragement and support of our research work

Funding

This research did not receive a specific grant from any funding agency in the public, commercial, or not-for-profit sectors.

Conflicts of Interest

No conflicts of interest exist.

Biographies

Marwan Zuhair Elias

Department of Medical Physics, College of Science, Mosul University, Mosul, Iraq, 009647702028210, marwanzuhairelias.1001@gmail.com

Marwan is an Iraqi lecturer and researcher specializing in Semiconductor Nanophysics. He earned his B.Sc. in Physics in 1993, followed by a M.Sc. in 1996 and a Ph.D. in 2010, all from the University of Mosul. His research focuses on the electronic, optical, and structural properties of nanomaterials, with an emphasis on their applications in medical and energy technologies. He has published over 20 peer-reviewed articles and continues to contribute to the advancement of nanoscale science and its real-world applications.

ORCID: 0000-0001-6521-3136

References

Barseghyan, M.G., Hakimyfard, A., Zuhair, M., Duque, C.A. and Kirakosyan, A.A. (2011). Binding energy of hydrogen-like donor impurity and photoionization cross-section in lnAs Pöschl–Teller quantum ring under applied magnetic field. *Physica E: Low-dimensional Systems and Nanostructures*, **44**(2), 419–24. DOI: 10.1016/j.physe.2011.09.013

Bhat, B.M.U.D. and Shah, K.A. (2018). Effect of dot size on exciton energy states confined in a spherical gallium arsenide quantum dot. *Nanosystem, Nanomaterial, Nanotechnology*, **16**(1), 175–9. DOI: 10.15407/nnn.16.01.175

Chafai, A., Essaoudi, I., Ainane, A., Dujardin, F. and Ahuja, R. (2019). Binding energy of an exciton in a GaN/AlN nanodot: Role of size and external electric field. *Physica B: Condensed Matter*, **559**(n/a), 23–8. DOI: 10.1016/j.physb.2019.01.047

Duque, C.A., Porras-Montenegro, N., Barticevic, Z., Pacheco, M. and Oliveira, L.E. (2006). Effects of applied magnetic fields and hydrostatic pressure on the optical transitions in self-assembled InAs/GaAs quantum dots. *Journal of Physics: Condensed Matter*, **18**(6), 1877. DOI: 10.1088/0953-8984/18/6/005

Elias, M.Z. (2019). Scattering by interface roughness of InAs/GaAs quantum well under some external influences. *Physica E: Low-dimensional Systems and Nanostructures*, **108**(n/a), 96–9. DOI: 10.1016/j.physe.2018.12.011

Fratelli, A., Zaffalon, M.L., Mazzola, E., Dirin, D.N., Cherniukh, I., Otero-Martínez, C. and Brovelli, S. (2025). Size-Dependent multiexciton dynamics governs scintillation from perovskite quantum dots. *Advanced Materials*, **37**(5), 2413182. DOI: 10.1002/adma.202413182

Ghosh, O.S.N., Gayathri, S., Allam, S.R., Sharan, A., Lal, S.S., Reddy, M.J.K. and Viswanath, A.K. (2024). Bound exciton engineering approach for tuning the thermal lensing phenomenon in anatase TiO2: Gd nanosystems. *Chemical Physics Impact*, **9**(n/a), 100679. DOI: 10.1016/j.chphi.2024.100679

Hsiao, T.K., Cova Fariña, P., Oosterhout, S.D., Jirovec, D., Zhang, X., van Diepen, C.J. and Vandersypen, L.M.K. (2024). Exciton transport in a germanium quantum dot ladder. *Physical Review X*, **14**(1), 011048. DOI: 10.1103/PhysRevX.14.011048

Janssens, K.L., Partoens, B. and Peeters, F.M. (2001a). Magnetoexcitons in planar type-II quantum dots in a perpendicular magnetic field. *Physical Review B*, **64**(15), 155324. DOI: 10.1103/PhysRevB.64.155324

Janssens, K.L., Partoens, B. and Peeters, F.M. (2002). Magneto‐exciton in single and coupled type ii quantum dots. *Physica Status Solidi (A)*, **190**(2), 571–6. DOI: 10.1002/1521-396X(200204)190:2<571::AID-PSSA571>3.0.CO;2-K

Janssens, K.L., Partoens, B. and Peeters, F.M. (2004). Magnetoexciton in vertically coupled InP/ GaInP quantum disks: Effect of strain on the exciton ground state. *Physical Review B—Condensed Matter and Materials Physics*, **69**(23), 235320. DOI: 10.1103/PhysRevB.69.235320

Janssens, K.L., Peeters, F.M. and Schweigert, V.A. (2001b). Magnetic-field dependence of the exciton energy in a quantum disk. *Physical Review B*, **63**(20), 205311. DOI: 10.1103/PhysRevB.63.205311

Kita, T., Harada, Y. and Asahi, S. (2019). Fundamentals of semiconductors. In: *Energy Conversion Efficiency of Solar Cells. Green Energy and Technology*. Springer, Singapore. DOI: 10.1007/978-981-13-9089-0_8

Kramar, V.M. (2009). Temperature dependence of the excitonic transition energy in flat semiconductor nanofilms. Ukr. J. *Phys.*, **54**(12), 1225–33.

Niehues, I., Blob, A., Stiehm, T., de Vasconcellos, S.M. and Bratschitsch, R. (2019). Interlayer excitons in bilayer MoS 2 under uniaxial tensile strain. *Nanoscale*, **11**(27), 12788–92. DOI: 10.1039/C9NR03332G

Niehues, I., Marauhn, P., Deilmann, T., Wigger, D., Schmidt, R., Arora, A. and Bratschitsch, R. (2020). Strain tuning of the Stokes shift in atomically thin semiconductors. *Nanoscale*, **12**(40), 20786–96. DOI: 10.1039/D0NR04557H

Pokutnyi, S.I. (2013). Binding energy of the exciton of a spatially separated electron and hole in quasi-zero-dimensional semiconductor nanosystems. *Technical Physics Letters*, **39**(n/a), 233–5. DOI: 10.1134/S1063785013030139

Pokytnyi, S.I., Gayvoronsky, V.Y. and Poroshin, V.N. (2023). Spatially indirect excitons and exciton quasimolecules in nanosystems with double quantum dots. *Molecular Crystals and Liquid Crystals*, **752**(1), 103–11. DOI: 10.1016/j.rinp.2025.108191

Wang, X., Gao, Y., Liu, X., Xu, H., Liu, R., Song, J. and Fan, F. (2024). Strong high-energy exciton electroluminescence from the light holes of polytypic quantum dots. *Nature Communications*, **15**(1), 6334. DOI: 10.1038/s41467-024-50432-8

Zieliński, M., Gołasa, K., Molas, M.R., Goryca, M., Kazimierczuk, T., Smoleński, T. and Babiński, A. (2015). Excitonic complexes in natural InAs/GaAs quantum dots. *Physical Review B*, **91**(8), 085303. DOI: 10.1103/PhysRevB.91.085303

Zuhair, M. (2012). Hydrostatic pressure and electric-field effects on the electronic and optical properties of InAs spherical layer quantum dot. *Physica E: Low-dimensional Systems and Nanostructures*, **46**(n/a), 232–5. DOI: 10.1016/j.physe.2012.09.017

Zuhair, M., Manaselyan, A. and Sarkisyan, H. (2009). Magneto-and electroabsorption in narrow-gap InSb cylindrical layer quantum dot. *Physica E: Low-dimensional Systems and Nanostructures*, **41**(8), 1583–90. DOI: 10.1016/j.physe.2009.05.002.